This article has been accepted for publication in IEEE/OSA Journal of Lightwave Technology. This is the author's version which has not been fully edited and content may change prior to final publication. Citation information: DOI 10.1109/JLT.2024.3398561

Finite-Genus Solutions-based Optical Communication with the Riemann-Hilbert Problem Transmitter and a Convolutional Neural Network Receiver

Stepan Bogdanov, Dmitry Shepelsky, Morteza Kamalian-Kopae, Anastasiia Vasylchenkova, and Jaroslaw E. Prilepsky

***Abstract*—In the study, we develop a new optical communication system based on the nonlinear Fourier transform for generic (quasiperiodic) finite-genus solutions to the nonlinear Schrödinger equation. At the transmitter, the finite-genus solutions of a generic type, which are not subject to any periodicity constraint, are generated by means of the Riemann-Hilbert problem (RHP) approach and utilized as the data carriers. Data encoding is achieved by modulating the phases of these solutions (as defined by the RHP), whereas the main spectrum determines signal parameters such as duration, bandwidth, and power. To decode the phases and compensate for their evolution, we propose a receiver that employs a convolutional neural network (CNN). CNN helps us overcome the lack of a complete theoretical framework for generic finite-genus solutions. We carry out the numerical simulations of a communication system that utilizes the phases of finite-genus solutions as data carriers with a CNN-based receiver. We present an analysis of the system's performance in terms of bit error ratio (BER) in dependence on signal power, propagation distance, and sampling rate. Additionally, we investigate the ability of the CNN-based receiver to process signals with a truncated linear spectrum to provide higher spectral efficiency, attaining $4.28\,\mathrm{bits/s/Hz}$ (for a single polarization) at $1040\,\mathrm{km}$ transmission distance.**

***Index Terms*—Convolutional neural network, fibre-optic communications, finite-genus solutions, nonlinear Fourier transform, Riemann-Hilbert problem.**

I. Introduction

THE development of inverse scattering transform (widely known as nonlinear Fourier transform (NFT) in recent optical communications literature) for the integration of a certain class of nonlinear evolutionary equations and, in particular, for the lossless nonlinear Schrödinger equation (NLSE) [1], opened up the possibility of using the NFT to compensate for both nonlinearity and dispersion in fibre-optic systems [2], [3]. The first work exploiting this idea was the proposition of the so-called eigenvalue communications by Hasegawa and Nyu [4]. In short, NFT is a technique to transform the nonlinear signal evolution governed by the NLSE into a linear evolution of special nonlinear spectral data (nonlinear Fourier spectrum) within the nonlinear Fourier (NF) domain. The NFT-based transmission techniques harness the aforementioned linearity of the nonlinear spectrum evolution as we directly modulate the solution parameters inside the NF domain [3]. Fibre-optic communications based on NFT has been developed using various methods: continuous nonlinear spectrum modulation [5]–[7], discrete components (solitons) modulation [8]–[13], full spectrum modulation [14]–[16], b-modulation of the continuous spectrum [17]–[20], and periodic NFT [21]–[23].

Despite the comprehensive efforts of numerous research groups, it is still challenging to make the NFT approach a practical solution [24]. In particular, the complexity of the NFT algorithms remains one of the major factors in limiting the method's applicability: some advanced approaches [25], [26] offer the algorithms with $N \log^2 N$ computational complexity (with N being the number of samples in a signal) for the direct and inverse problems processing the signals with continuous spectrum only. However, their performance substantially degrades as power increases because a higher value of N is required to provide satisfying accuracy [27].

Among other NFT techniques, periodic NFT (PNFT) has been proposed [3], [28] to alleviate some difficulties of the "conventional" NFT-based transmission systems [29]. The PNFT can be understood as a nonlinear analog of conventional linear OFDM communication. Although the PNFT offers several advantages over the conventional NFT – including continuous signal transmission as opposed to burst mode, smaller processing window at the receiver, and full control over the signal's duration, bandwidth, and power – there is no satisfying analysis of such systems, primary due to the complex mathematical theory behind the approach. The implementation of PNFT-based transmission systems has been investigated using the algebro-geometric approach [22], [23] where the data were mapped onto the main spectrum of finite-genus solutions, whereas the algebro-geometric formalism was used to generate modulated signals at the transmitter through evaluation of the Riemann theta functions [30], [31]. The Riemann-Hilbert problem (RHP) approach is an alternative and, from our viewpoint, somewhat computationally simpler

Stepan Bogdanov and Jaroslaw E. Prilepsky acknowledge Leverhulme Trust project, Grant No. RPG-2018-063.

Stepan Bogdanov, Jaroslaw E. Prilepsky, and Morteza Kamalian-Kopae are with Aston Institute of Photonic Technologies, Aston University, Birmingham, B4 7ET, UK (Stepan Bogdanov's email 190244042@aston.ac.uk).

Dmitry Shepelsky is with B. Verkin Institute for Low Temperature Physics and Engineering, Kharkiv, 61103, Ukraine, and V. Karazin Kharkiv National University, Kharkiv, 61022, Ukraine.

Anastasiia Vasylchenkova is with University College London, Gower Street, London, WC1E 6BT, UK.

We used ChatGPT-4 and Grammarly for grammar correction in the manuscript preparation stage.

technique: it is based on an analytic factorization problem in the nonlinear Fourier domain [29], [32], [33]. However, the optical communication approaches highlighted above suffer from a technical drawback: they are constrained to employ *perfectly periodic signals*, reducing the flexibility of the methods and adding some computational complexity at the signal generation stage. As a result, both methods operate within a quasi-linear regime, omitting the consideration of actual nonlinear dynamics of finite-genus solutions.

The present study continues the development of the approach detailed in [32]. The communication system proposed in this research is based on data transmission using non-periodic finite-genus solutions to the NLSE. Information is modulated onto the associated spectral parameters (by solving the inverse NFT problem at the transmitter formulated as an RHP) with a finite-genus solution. This evolved solution (the signal at the receiver) then has to be processed for retrieving the information from the spectral data (and thus to recover the initial information sent from the transmitter) through solving the corresponding direct problem. However, when solving the direct problem to demodulate the data in this setting in our previous research, we faced some technical limitations [32]: (i) signals must be strictly periodic, which significantly restricts the variety of scattering data configurations; (ii) symbols have to include a cyclic extension to compensate for the dispersion broadening, thereby decreasing the achievable time-bandwidth product; (iii) phases of the nonlinear modes were defined on the interval from 0 to π, which is only half of the possible range. Further, the latter constraint was overcome by formulating an analytical approach capable of retrieving the phases of periodic finite-genus solutions without restrictions on their values [34]; however, this approach turned out to be very computationally involved.

Relaxing the periodicity condition helps with the deficiencies of the previously proposed systems. However, this requires building a fundamentally new mathematical approach to receiving data in non-periodic finite-genus optical systems. In our approach here, we have implemented machine learning techniques, harnessing the power of convolutional neural networks (CNN).

Artificial neural networks (NN) have demonstrated their outstanding potential in application to various areas of fibre-optic communications. For example, we mention many works dedicated to the NN-based equalization problem [35]–[37]. Recently, some works have focused on applications within the NFT-based optical transmission [10], [38]–[40], and on the systems based on the PNFT [41]. Furthermore, in [42], some of the present authors developed a pioneering CNN-based approach to determine the phases of finite-genus solutions; therefore, extending the latter approach to improve the respective optical communication systems looks natural.

This work presents a fibre-optic communication system that utilizes the NFT for finite-genus solutions to the NLSE. At the transmitter (Tx), we modulate the phases of finite-genus solutions and employ the RHP approach to generate a time-domain signal $q(t)$. At the receiver (Rx), we adopt a CNN-based method, as detailed in [42], to demodulate the signal, detect the phases, and compensate for their evolution. Previously, we proposed these ideas in [43], where a convolutional neural network was applied to detect received information in the system with an ideally distributed amplification. In the current paper, we aim to evaluate the performance of realistic fibre-optic communication systems based on finite-genus solutions with lumped amplification. For the first time, we are employing finite-genus solutions of a generic type, eliminating periodicity constraints, and go to much higher powers compared to the previous studies.

II. The Riemann-Hilbert problem and finite-genus solutions

The focusing NLSE governing signal propagation over an optical fibre with anomalous dispersion, given in the dimensionless form, is:

$$iq_z + q_{tt} + 2|q|^2 q = 0, \tag{1}$$

where z is the evolutionary variable, t is the time variable, and $q(t,z)$ represents the signal envelope. The equation describes the signal propagation over a single polarization in a lossless and noiseless scenario.

The NLSE has a class of solutions known as finite-genus solutions (also referred to as finite-band or finite-gap solutions in various literature). A genus-N solution $q(t,z)$ can be parameterized through a set of spectral data. A possible way to do this is to exploit the RHP formalism. Namely, q is given by $q(t,z) = 2i\lim_{\lambda\to\infty}\lambda M_{12}(t,z,\lambda)$, where $M(t,z,\lambda)$ is the solution of the RHP formulated as follows: given the complex-valued parameters $\{\lambda_j\}_{j=0}^N$ (termed the *main spectrum*) and the real-valued parameters $\{\phi_j\}_{j=0}^N$, $\phi_j \in [0,2\pi)$ (termed the *phases*), find $M(t,z,\lambda)$ which is a 2×2-valued function satisfying the following conditions:

- for any t and z, $M(t,z,\lambda)$ is analytic, as function of λ, in $\mathbb{C}\setminus\Gamma$, where $\Gamma = \cup_{j=0}^N \Gamma_j$ and $\Gamma_j = (\lambda_j, \lambda_j^*)$ (the arc connecting λ_j with its complex conjugate λ_j^*);
- the limiting values $M_\pm(t,z,\lambda)$ of $M(t,z,\lambda)$ as $\lambda\in\Gamma$ is approached from the left or from the right are related by
$$M_+(t,z,\lambda) = M_-(t,z,\lambda)J(t,z,\lambda), \quad \lambda\in\Gamma, \tag{2}$$
where
$$J(t,z,\lambda) = \begin{pmatrix} 0 & ie^{-i(\phi_j+2i\lambda t+4i\lambda^2 z)} \\ ie^{i(\phi_j+2i\lambda t+4i\lambda^2 z)} & 0 \end{pmatrix},$$
$\lambda\in\Gamma_j$, $j=0,\ldots,N$;
- $M(t,z,\lambda)\to I$ (identity matrix) as $\lambda\to\infty$.

The construction of $q(t,z)$ in terms of the solution of the RHP involving $\{\lambda_j\}_{j=0}^N$ and $\{\phi_j\}_{j=0}^N$ as the input data can be interpreted as an *inverse problem*; in turn, the associated *direct problem* consists in the following: given a genus-N solution $q(t,z)$ as function of t evaluated at a particular value of z, retrieve the underlying parameters $\{\lambda_j\}_{j=0}^N$ and $\{\phi_j\}_{j=0}^N$.

Importantly, $q(t,z)$ characterized as above can be equivalently given in terms of the solution of another RHP, where the matrix $J(t,z,\lambda)$ in the jump condition (2) is replaced by

$$\hat{J}(t,z,\lambda) = \begin{pmatrix} 0 & ie^{-i(\phi_j+C_f^j t+C_g^j z)} \\ ie^{i(\phi_j+C_f^j t+C_g^j z)} & 0 \end{pmatrix},$$

$\lambda \in \Gamma_j$, $j = 0, \ldots, N$, where the real-valued C_f^j and C_g^j are uniquely determined by the main spectrum alone and represent the temporal and propagation frequencies. For more details see [29], [32], [33]. We associate the contribution of each pair $\{\lambda_j, \lambda_j^*\}$ to the signal $q(t, z)$ with the corresponding *nonlinear mode*. In this context, the frequency C_f^j and the phase ϕ_j are attributes of the j-th nonlinear mode of the signal.

In specific scenarios where the frequencies $\{C_f^j\}_{j=0}^N$ are commensurable, the resulting solution is periodic, and the direct problem can be addressed using the monodromy matrix formalism [25], [32], where the points $\{\lambda_j, \lambda_j^*\}$ re-appear as the main spectrum. In the general case where the frequencies $\{C_f^j\}_{j=0}^N$ are non-commensurable, in what follows we still use the notion of "main spectrum" for the contours' end points in the RHP formalism of the inverse problem. It is the fact that there is no established analytical approach to solve the direct problem in the general case that motivated us to use a convolutional neural network for the direct problem, i.e. the problem of retrieving $\{\phi_j\}_{j=0}^N$ (assuming that $\{\lambda_j\}_{j=0}^N$ are fixed and known) from the associated solution to the NLSE taken as a function of t at a fixed z.

The RHP formalism allows linearizing the evolution: the main spectrum remains unchanged while signals propagate through an optical fibre whereas the evolution of the phases follows a simple linear relation:

$$\phi_j(z) = \phi_j(0) + (C_g^j - 2g_0)z, \tag{3}$$

where z denotes the propagation distance and g_0, similarly to C_g^j, is determined by the main spectrum alone [29], [32].

III. Finite-genus solutions-based communication system

At the core of our research is the idea of using the properties of finite-genus solutions to develop an effective communication system. These properties include: (i) the trivial evolution of scattering data (3), the property that lies behind the NFT; (ii) absence of burst mode operation that potentially increases time-bandwidth product and reduces the impact of noise; (iii) full control over signal duration, bandwidth, and power by manipulating the main spectrum. These properties of finite-genus solutions make them a promising candidate to carry data in fibre-optic communications.

Data transmission utilizing finite-genus solutions involves the following stages: (i) encoding information onto the phases of finite-genus solutions; (ii) given the main spectrum, determined by the desired signal parameters and phases, generating $q(t, z)$ with the RHP solver; (iii) transmitting the signals through an optical fibre; (iv) and retrieving the phases with a convolutional neural network-based receiver. This receiver compensates for the evolution of the phases and solves the direct problem of retrieving their values. The schematic of the communication system is illustrated in Fig. 1.

In order to build a proof-of-concept system and demonstrate the feasibility of finite-genus communications, we utilize genus-4 solutions to the NLSE to encode information into their phases. Genus-4 solutions are chosen because their genus is high enough to demonstrate complex nonlinear dynamics

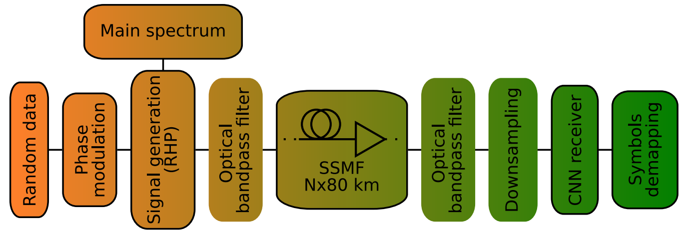

Fig. 1: Communication system consisting of phase modulation and signal generation at the transmitter (with power, duration, and bandwidth defined by the main spectrum), N spans of an optical fibre with EDFA amplification, and phase retrieval at the receiver. Optical bandpass filters at the transmitter and receiver and downsampling are not used in all simulations and depicted without frames in the scheme.

but, at the same time, they can be calculated by means of existing algorithms effectively. We observed the nonlinear dependence of the signal's duration and bandwidth on the real and imaginary parts of the main spectrum for genus-4 solutions. This confirms that the signals we choose to operate with indeed demonstrate the nonlinear character of their evolution. The main spectrum configuration we employ is as follows:

$$\lambda = \{-2 + ai, -1 + ai, ai, 1 + ai, 2 + ai\}. \tag{4}$$

Both the real and imaginary parts of the main spectrum determine a signal's duration T and bandwidth W. However, in the linear limit, when $a << 1$, the influence of the nonzero parameter a diminishes, and both T and W are determined by the real part of the main spectrum only. It is worth mentioning that the phases also affect the bandwidth of a signal. As a signal propagates through an optical fibre, its envelope undergoes changes, as well as its linear spectrum, that can be attributed to the phases only because the main spectrum remains constant. For the main spectrum given in (4) with a specific value of a, we calculate the frequency for each nonlinear mode ($C_f^1, C_f^2 ...$) and define the signal's duration as $T = 2\pi / C_f^{min}$, where $C_f^{min} = \min_j C_f^j$ (as defined in Section II). The smallest frequency corresponds to the maximum period across all nonlinear modes. So, we can be sure that the signal with duration T contains at least one period of each nonlinear mode, see Fig. 2 where the maximum period T_1 corresponds to the minimum frequency C_f^{min}. Therefore, all essential information is encapsulated within the segment of the signal lasting T_1, defining the symbol duration $T = T_1$. While the parameter a modulates the power of signals, due to the nonlinear nature of finite-genus solutions, it also influences the frequencies C_f^j.

The information signal consists of a sequence of genus-4 symbols, each having a duration of T as previously defined. We concatenate these symbols together into a sequence without guard intervals and transmit it over a single polarization and one frequency channel. Typically, in such systems, there is an extension of the symbols beyond the period T to prevent their overlapping due to chromatic dispersion broadening. However, in our approach, instead, there is no signal extension:

This article has been accepted for publication in IEEE/OSA Journal of Lightwave Technology. This is the author's version which has not been fully edited and content may change prior to final publication. Citation information: DOI 10.1109/JLT.2024.3398561

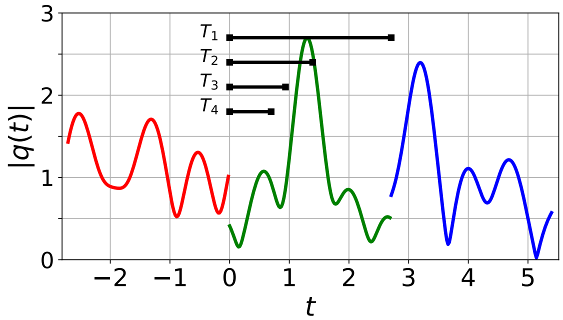

Fig. 2: Three consecutive genus-4 symbols at the transmitter calculated for the main spectrum given by (4) with $a = 0.6$ and random phases from the modulation set. The period of each nonlinear mode (T_1, T_2, T_3, T_4) for the central symbol is depicted to demonstrate that the maximum period T_1 contains all others.

we put symbols one by one, see Fig. 2. Compensation for any dispersion-induced overlap is managed by our CNN-based receiver, which processes not only the current symbol but also its neighboring ones. The symbols are arranged closely in sequence, with no temporal gaps between them. However, there are discontinuities in amplitude and phase among adjacent symbols. Each discontinuity can be mitigated by sacrificing one of the five phases employed in modulation that reduces the system capacity and, therefore, is not adopted. So, we do not apply any technique to resolve these disruptions, relying on our CNN receiver.

The evolution of the finite-genus solutions propagated over optical fibre is dictated by the NLSE, as given in (1). This model describes signal propagation in the medium with chromatic dispersion and nonlinearity only. Introducing periodic attenuation and amplification deviates from these conditions and breaks the integrability of the system: the theory of finite-genus solutions, as well as their linear evolution of the phases (3), does not hold rigorously. While any deviations from the original model make the dynamics of the signals more intricate, their propagation averaged over many spans of optical fibre remains governed by (1), often referred to as the lossless path-averaged model [6].

Convolutional neural network-based receiver

A key component of the receiver is CNN: its architecture is similar to that of Ref. [44]. The approach is detailed in Refs. [42], [43], where it has been used for retrieving the phases of finite-genus solutions. In this study, we expand the NN functionality: Beyond retrieving the phases of the received symbols, it also compensates for their evolution as dictated by (3). The network was trained on data propagated through the optical fibre given at the receiver with the transmitter phases as labels. The neural network architecture can be described as follows: it comprises three convolutional layers followed by a fully connected layer, as illustrated in Fig. 3. The hyperparameters were optimized by Bayesian methods [45]. Their resulting values are cataloged in Table I. For a more comprehensive discussion on the implementation of the CNN, one can refer to [42].

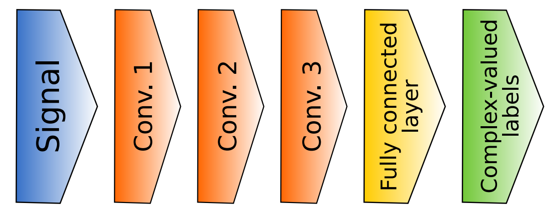

Fig. 3: Scheme of the CNN-based receiver consisting of three convolutional layers followed by a fully connected and output layer.

TABLE I: The hyperparameters of the CNN at the receiver with the architecture given in Fig. 3.

	Filters	Kernel size	Activation
1 conv.	94	3	tanh
2 conv.	112	17	tanh
3 conv.	145	18	sigmoid
Fully con.	128 neurons		sigmoid

The receiver processes signals after propagation through an optical fibre. It takes three consecutive symbols at the input at two sample rates, 64 and 128 samples per symbol, and retrieves the phases of the central symbol. We determined that processing three symbols suffices to account for dispersion-induced memory. Consequently, we do not implement any linear chromatic dispersion compensation when feeding signals into the CNN-receiver. We use the following equation to estimate the broadening of signals [6]:

$$\Delta T = 2\pi|\beta_2|BL, \tag{5}$$

where $\beta_2 = -21.67\,\mathrm{ps}^2/\mathrm{km}$ is the chromatic dispersion, $B = 6\,\mathrm{GHz}$ is a typical bandwidth of the signal of the presented communications system (one among others), $L = 1040\,\mathrm{km}$ is the propagation distance. By substituting the given values into the equation, we find the broadening of the signal $\Delta T = 0.85\,\mathrm{ns}$, whereas the symbol's duration is $1\,\mathrm{ns}$. So, we guarantee that three consecutive symbols contain all information about the central one among them. Moreover, it was mentioned in [23] that finite-genus solutions show less broadening in comparison with the linear estimate (5) due to the nonlinear nature of their evolution.

To train the CNN, we compiled a dataset comprising $400\,000$ training symbols and at least $20\,000$ test symbols. In some experiments, we expanded the test dataset to ensure statistically significant results. The test dataset was not utilized during training. For labeling, we employed complex-valued points on unit circles that correspond to phases. This labeling approach was adopted to guarantee the periodicity of the labels corresponding to the phase periodicity of the solutions. Therefore, the CNN predicted points on the unit circle that matched the phases. These points were used to apply the 'hard decision' technique. The network was trained over $5\,000$ epochs using the Adam optimizer (learning rate 10^{-4}) within the TensorFlow 2.0 framework.

IV. Results

We numerically simulate the propagation of signals within the communication system illustrated in Fig. 1. We encode data onto the phases of finite-genus solutions and generate signals $q(t, z)$ by concatenating symbols to form sequences of 1020 symbols each. These signals are then transmitted through a communication line, which consists of multiple spans of optical fibre, each 80 km in length (the exact number of spans varies in our simulations), with an EDFA amplification scheme over one frequency channel and noise added at the end of each span. After propagation, the first and the last ten symbols in sequences are removed to avoid any boundary effects. We apply the CNN-based receiver detailed above (and independently trained for each set of parameters: power, propagation distance, bandwidth) and evaluate the system performance by calculating the bit error rate (BER), which is determined by directly counting the erroneous bits in the received sequences.

Specifically, to generate information-bearing symbols, we employ the main spectrum configuration as in (4). The symbols' duration and bandwidth are determined primarily by the real part of the main spectrum. At the same time, due to the nonlinear nature of signals, the imaginary part (parameter a) affects the duration and bandwidth as well. The signals' power is also modulated by a. We normalize the duration of all symbols to $1\,\mathrm{ns}$ regardless of the value of a (the detailed normalization procedure is given in [3]). We implement a 32-phase shift keying (PSK) modulation for each phase of the genus-4 solution (5 phases), inset in Fig 4.

We simulate the propagation of signals through standard single mode fibre (SSMF) with the following parameters: group velocity dispersion $\beta_2 = -21.67\,\mathrm{ps}^2/\mathrm{km}$, nonlinearity coefficient $\gamma = 1.27 \times 10^{-3}\,\mathrm{mW}^{-1}\mathrm{km}^{-1}$, and attenuation $\alpha = 0.2\,\mathrm{dB/km}$. We employ the split-step Fourier method (SSFM), having 128 samples of the temporal variable per symbol and 128 steps of the evolutionary variable per fibre span [46]. We add the Gaussian white noise at the end of each span with the spectral power density $N_{ASE} = (e^{\alpha L_A} - 1) h\nu_s NF/2$, where $L_A = 80\,\mathrm{km}$ is the span length, $h\nu_s$ represents the photon energy (with h being Planck constant and carrier's frequency $\nu_s = 193.4\,\mathrm{THz}$) and $NF/2$ being a noise figure per polarization [46], $NF = 10^{4.5/10}$.

We evaluate the system performance as a function of launch power, examining the BER as shown in Fig. 4. Ranging parameter a from 0.4 to 2 corresponds to a launch power from $-4\,\mathrm{dBm}$ to $3\,\mathrm{dBm}$. We consider receiving at two sampling rates: 128 and 64 samples per symbol (that corresponds to $128\,\mathrm{GSam/s}$ and $64\,\mathrm{GSam/s}$), these two options are exploited to estimate the performance of the receiver at a practical sample rate $64\,\mathrm{GSam/s}$ and investigate how this performance can be enhanced with an increased value. We demonstrate the data signaling below the forward error correction (FEC) threshold, which has a value of 3.8×10^{-3} and an overhead of 7% for both sampling rates [47]. The optimal launch power yielding the lowest BER for $128\,\mathrm{sam/sym}$ is $-1.72\,\mathrm{dBm}$ ($a = 0.6$), whereas, for $64\,\mathrm{sam/sym}$, it is $-0.57\,\mathrm{dBm}$ ($a = 0.75$). The behavior of the BER curve for $128\,\mathrm{sam/sym}$ at the lower power levels deviates below the expected position. This can be attributed to the CNN's inherent ability to filter noise, a feature also discussed in [44]. Thus, the higher dimensionality of the CNN's input affords improved noise filtering.

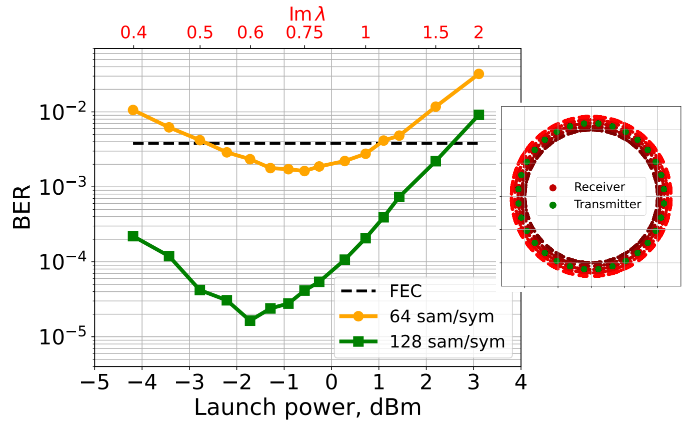

Fig. 4: BER is plotted as a function of launch power for $128\,\mathrm{sam/sym}$ (depicted in green) and $64\,\mathrm{sam/sym}$ (depicted in yellow) in comparison with the FEC threshold of 3.8×10^{-3} (7% overhead). On the upper axis, the corresponding values of the imaginary part of the main spectrum, parameter a, are indicated (as defined in (4)). The inset displays the constellation diagram at the receiver for optimal power of $64\,\mathrm{sam/sym}$ scenario, as well as reference values at the transmitter. The five-layer structure of the output clouds (represented by shades of red from dark to light) corresponds to the received phases for different nonlinear harmonics of 4-genus solutions.

For the power levels that provide the lowest BER (which are different for $128\,\mathrm{sam/sym}$ and $64\,\mathrm{sam/sym}$, as indicated in Fig. 4), we evaluate the performance of our transmission system as a function of the number of spans, as shown in Fig. 5. We demonstrate that receiving at $128\,\mathrm{sam/sym}$ can maintain a BER below the FEC threshold up to 23 spans, which corresponds to a total distance of $1840\,\mathrm{km}$. At the same time, the maximum distance achievable for $64\,\mathrm{sam/sym}$ receiving is 15 spans, equating to $1200\,\mathrm{km}$.

The linear spectrum of the signal (1020 symbols) for $a = 0.75$ at the transmitter is depicted in Fig. 6. This value of the parameter a corresponds to the optimal power (providing minimum BER) for $64\,\mathrm{sam/sym}$ sampling rate receiving. The spectrum contains overtone-like structures with a non-negligible part of the energy therein. Bandwidth corresponding to 99% of energy equals to $21\,\mathrm{GHz}$, using of which is absolutely ineffective. At the same time, our tailor-designed receiver is able to process signals slightly deviated from exact finite-genus solutions. So, we apply a narrow-band filter at the transmitter to cut only the substantial part of the signal linear spectrum as given in Fig. 6. The central part still contains the majority of energy (95%) and provides the properties of finite-genus solutions to be saved. At the receiver, we also apply the same narrow-band filter to clean the signal from noise.

To investigate the properties of the signals with the truncated spectrum, we consecutively add overtones in the bandwidth starting from zero and going up to five overtones on each side

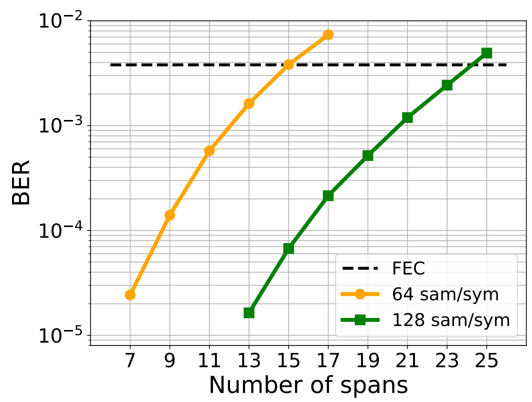

Fig. 5: BER as a function of distance given in the number of spans (each $80\,\mathrm{km}$ in length) for $128\,\mathrm{sam/sym}$ (in green) and $64\,\mathrm{sam/sym}$ (in yellow) in comparison with the FEC threshold of 3.8×10^{-3} (7% overhead).

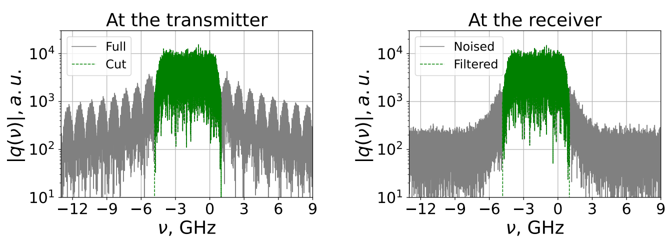

Fig. 6: Left: the linear spectrum at the transmitter for optimal $a = 0.75$ of $64\,\mathrm{sam/sym}$ scenario before (grey) and after (green) cutting overtones. Right: the same spectrum at the receiver before (grey) and after (green) filtering of noise.

of the spectrum, Fig. 6. Adding overtones to the spectrum decreases the effect of distortion because of less deviation from exact finite-genus signals but increases the time-bandwidth product due to the wider spectrum. At the same time, a bigger bandwidth contains more noise that distorts signals. We calculate BER as well as spectral efficiency (SE) varied with the number of overtones for receiving at $64\,\mathrm{sam/sym}$ with total distance $1040\,\mathrm{km}$ (13 spans), Table II. The SE can be estimated for our communication system as the following:

$$SE = \frac{5 \times AIR_{av}}{T_s \times B}, \tag{6}$$

where T_s is the duration of the symbol, and B is the bandwidth (varied with the number of overtones in the spectrum). AIR_{av} is the achievable information rate per one nonlinear mode averaged over all nonlinear modes in a symbol and over all symbols in a signal. So, $5 \times AIR_{av}$ gives the achievable information rate per symbol (each symbol contains 5 modes). We calculated AIR_{av} according to the technique based on the assumption about the Gaussian statistics of the received symbols [48].

We observe that reducing the number of overtones in the signal spectrum provides better performance because of effective filtering of noise (compare with the $\mathrm{BER} = 1.63 \times 10^{-3}$ in the scenarios when the full bandwidth without any truncation is used, Fig. 4). The ultimate cut-off of overtones, a scenario when only the central part of the spectrum is saved, slightly increases BER because deviation from the exact finite-genus solutions is getting sufficient. Nevertheless, the last scenario still provides signaling with the applicable BER, while the achieved SE efficiency is $4.28\,\mathrm{bits/s/Hz}$. With a symbol rate $1\,\mathrm{Gbaud}$, the total capacity of our one-channel one-polarization system is $25\,\mathrm{Gbits/s}$. However, this capacity can be enhanced by exploiting a wider bandwidth in comparison with $5.83\,\mathrm{GHz}$ in our case. This can be achieved either by increasing the genus of solutions or filling the bandpass with many channels of the type we considered in this study. Simply decreasing the symbol duration T necessitates a higher sampling rate (that is impractical) to maintain the same number of samples per symbol (64 or 128) for which the properties of the CNN receiver are analyzed.

TABLE II: Bandwidth, spectral efficiency (SE), and BER for the transmission with a truncated spectrum.

Number of overtones	0	1	2	3	4	5
Bandwidth, GHz	5.83	7.95	9.96	11.96	13.95	15.97
SE, bits/s/Hz	4.28	3.14	2.51	2.09	1.79	1.56
BER, $\times 10^{-5}$	8.64	2.95	2.10	2.39	2.66	2.99

For comparative purposes, it is useful to mention some of the highest performances of other NFT-based communication systems. In the research [49], the performance of a b-modulation-based communication system was estimated. The system featured an improved receiver exploiting the statistical correlations between noise and information signals. For transmission parameters similar to those considered in our work, within a narrow-bandwidth system operating at $5\,\mathrm{GHz}$ over a propagation distance of $960\,\mathrm{km}$, the authors detected maximum SE equals to $5.51\,\mathrm{bits/s/Hz}$. In another research, a nonlinear frequency division multiplexing dual-polarization scheme was implemented employing the properties of Hermite-Gauss wave carriers [19]. They demonstrated a system with $4.75\,\mathrm{GHz}$ bandwidth, providing spectral efficiency of $12\,\mathrm{bits/s/Hz}$ over both polarizations for transmission distance $800\,\mathrm{km}$. Although our system has a lower SE, we can expect that systems based on finite-genus solutions have the potential to increase effectiveness further. Exploiting higher-genus solutions and sampling optimization may be the next steps in this direction.

V. Conclusion

In the study, we have developed an innovative method for data transmission based on finite-genus solutions to the nonlinear Schrödinger equation. We exploited the Riemann-Hilbert problem framework to generate signals at the transmitter of the communication system with one polarization while encoding data into the phases defined in the frame of RHP. At the receiver, the convolutional neural networks-based approach is applied to retrieve the phases and compensate for their evolution during transmission. A key novel idea of our method is to apply the CNN-based receiver, which allows us to overcome the constraints of exactly periodic NFT. This advancement eliminates the limitations imposed by the existing approaches based on RHP, such as the necessity of relying exclusively on periodic solutions and using cyclic extension, as well as expands the range of phases available for modulation in comparison with the method given in previous research [32]. Moreover, we employ CNN at the receiver, harnessing their ability to compensate for distortions in the system deviating from its ideal model and CNN's property to filter noise, thereby enhancing the communication system's performance. We implemented the described communication system as a proof-of-concept without additional optimizations, aiming to unlock the potential of finite-genus solutions in scenarios unrestricted by the limitations of preceding approaches.

Our simulations demonstrated the successful data transmission over a single frequency channel with BER below the 3.8×10^{-3} (7% overhead) FEC threshold with $128\,\mathrm{sam/sym}$ and $64\,\mathrm{sam/sym}$ sample rates. The system effectively transmitted data over distances of $1840\,\mathrm{km}$ (23 spans) and $1200\,\mathrm{km}$ (15 spans) for both sample rates correspondingly. Additionally, our investigation explored the system performance when operated with a truncated signal spectrum for $64\,\mathrm{sam/sym}$, aiming to improve spectral efficiency. While cutting the overtones-like parts of the spectrum off, we achieved the SE equal to $4.28\,\mathrm{bits/s/Hz}$ at $1040\,\mathrm{km}$ transmission distance.

Despite significant advances in previous research, several unresolved problems persist in applying finite-genus NFT in fibre-optic communications. An important area of focus is the development of algorithms for generating high-genus solutions [31]. The incorporation of high-genus solutions is critical for effective bandwidth utilization and enhancing spectral efficiency. Moreover, these algorithms must address the bottleneck of the NFT methods: the high computational complexity. Furthermore, to the best of our knowledge, a dual-polarization communication system employing finite-genus solutions has not yet been realized, partly due to the incomplete theory for the NFT methods for the dual-polarization Manakov channel. Addressing these challenges is crucial to improving the applicability of finite-genus solutions in fibre-optic communications and the efficiency of the resulting systems.

References

[1] V. Zakharov and A. Shabat, "Exact theory of two-dimensional self-focusing and one-dimensional self-modulation of waves in nonlinear media," *Sov. Phys. JETP*, vol. 34, no. 1, p. 62, 1972.

[2] M. I. Yousefi and F. R. Kschischang, "Information transmission using the nonlinear Fourier transform, Part I: Mathematical tools," *IEEE Transactions on Information Theory*, vol. 60, no. 7, pp. 4312–4328, 2014.

[3] S. K. Turitsyn, J. E. Prilepsky, S. T. Le, S. Wahls, L. L. Frumin, M. Kamalian, and S. A. Derevyanko, "Nonlinear Fourier transform for optical data processing and transmission: advances and perspectives," *Optica*, vol. 4, no. 3, pp. 307–322, 2017.

[4] A. Hasegawa and T. Nyu, "Eigenvalue communication," *Journal of lightwave technology*, vol. 11, no. 3, pp. 395–399, 1993.

[5] J. E. Prilepsky, S. A. Derevyanko, K. J. Blow, I. Gabitov, and S. K. Turitsyn, "Nonlinear inverse synthesis and eigenvalue division multiplexing in optical fiber channels," *Physical Review Letters*, vol. 113, no. 1, p. 013901, 2014.

[6] S. T. Le, J. E. Prilepsky, and S. K. Turitsyn, "Nonlinear inverse synthesis technique for optical links with lumped amplification," *Optics Express*, vol. 23, no. 7, pp. 8317–8328, 2015.

[7] S. A. Derevyanko, J. E. Prilepsky, and S. K. Turitsyn, "Capacity estimates for optical transmission based on the nonlinear Fourier transform," *Nature Communications*, vol. 7, no. 1, p. 12710, 2016.

[8] A. Maruta, "Eigenvalue modulated optical transmission system," *2015 Opto-Electronics and Communications Conference (OECC)*, pp. 1–3, 2015.

[9] S. Gaiarin, A. M. Perego, E. P. da Silva, F. Da Ros, and D. Zibar, "Dual-polarization nonlinear Fourier transform-based optical communication system," *Optica*, vol. 5, no. 3, pp. 263–270, 2018.

[10] S. Yamamoto, K. Mishina, and A. Maruta, "Demodulation of optical eigenvalue modulated signals using neural networks," *IEICE Communications Express*, vol. 8, no. 12, pp. 507–512, 2019.

[11] Y. Chen, M. Baniasadi, and M. Safari, "Neural network-aided receivers for soliton communication impaired by solitonic interaction," *Optics Express*, vol. 31, no. 26, pp. 43 289–43 306, 2023.

[12] Y. Bi, H. Xu, H. Gao, C. Bai, Y. Zhang, L. Xi, N. Cui, L. Yang, W. Sun, and X. Tang, "Frequency offset modeling in presence of ase noise and corresponding low-complexity solution for discrete spectrum modulated nonlinear frequency division multiplexing system," *Optics Communications*, vol. 537, p. 129396, 2023.

[13] T. Kodama, K. Mishina, Y. Yoshida, D. Hisano, and A. Maruta, "Transmission of hyper-multi-level eigenvalue-modulated signal using arbitrary optical multi-eigenvalue," *Optics Communications*, vol. 546, p. 129748, 2023.

[14] R. Zhang, L. Xi, J. Wei, J. Deng, S. Du, W. Zhang, X. Zhang, and X. Xiao, "Optimal design of eigenvalues for the full-spectrum modulated nonlinear frequency division multiplexing transmission system," *IEEE Photonics Journal*, 2023.

[15] S. T. Le, V. Aref, and H. Buelow, "Nonlinear signal multiplexing for communication beyond the kerr nonlinearity limit," *Nature Photonics*, vol. 11, no. 9, pp. 570–576, 2017.

[16] F. Da Ros, S. Civelli, S. Gaiarin, E. P. Da Silva, N. De Renzis, M. Secondini, and D. Zibar, "Dual-polarization nfdm transmission with continuous and discrete spectral modulation," *Journal of Lightwave Technology*, vol. 37, no. 10, pp. 2335–2343, 2019.

[17] T. Gui, G. Zhou, C. Lu, A. P. T. Lau, and S. Wahls, "Nonlinear frequency division multiplexing with b-modulation: shifting the energy barrier," *Optics Express*, vol. 26, no. 21, pp. 27 978–27 990, 2018.

[18] S. A. Derevyanko and J. E. Prilepsky, "Channel model for the dual-polarization b-modulated nonlinear frequency-division multiplexing optical transmission systems," *Optics Express*, vol. 31, no. 12, pp. 19 686–19 702, 2023.

[19] M. Balogun, S. Derevyanko, and L. Barry, "Dual-polarization Hermite-Gaussian-based NFDM transmission system," *IEEE Access*, vol. 11, pp. 125 692–125 697, 2023.

[20] X. Yangzhang, S. T. Le, V. Aref, H. Buelow, D. Lavery, and P. Bayvel, "Experimental demonstration of dual-polarisation NFDM transmission with b-modulation," in *2019 IEEE Photonics Conference (IPC)*. IEEE, 2019, pp. 1–4.

[21] M. Kamalian, J. E. Prilepsky, S. T. Le, and S. K. Turitsyn, "Periodic nonlinear Fourier transform for fiber-optic communications, Part II: eigenvalue communication," *Optics Express*, vol. 24, no. 16, pp. 18 370–18 381, 2016.

[22] J.-W. Goossens, H. Hafermann, and Y. Jaouën, "Data transmission based on exact inverse periodic nonlinear Fourier transform, Part I: Theory," *Journal of Lightwave Technology*, vol. 38, no. 23, pp. 6499–6519, 2020.

[23] J.-W. Goossens, Y. Jaouën, and H. Hafermann, "Experimental demonstration of data transmission based on the exact inverse periodic nonlinear Fourier transform," in *Optical Fiber Communication Conference*. Optica Publishing Group, 2019, pp. M1I–6.

[24] S. Civelli, E. Forestieri, and M. Secondini, "Why noise and dispersion may seriously hamper nonlinear frequency-division multiplexing," *IEEE Photonics Technology Letters*, vol. 29, no. 16, pp. 1332–1335, 2017.

[25] S. Wahls and H. V. Poor, "Fast numerical nonlinear Fourier transforms," *IEEE Transactions on Information Theory*, vol. 61, no. 12, pp. 6957–6974, 2015.

[26] S. Wahls and V. Vaibhav, "Fast inverse nonlinear Fourier transforms for continuous spectra of Zakharov-Shabat type," *arXiv preprint arXiv:1607.01305*, 2016.

[27] S. Wahls, S. Chimmalgi, and P. J. Prins, "Wiener-Hopf method for b-modulation," in *Optical Fiber Communication Conference*. Optica Publishing Group, 2019, pp. W2A–50.

[28] M. Kamalian, J. E. Prilepsky, S. T. Le, and S. K. Turitsyn, "Periodic nonlinear Fourier transform for fiber-optic communications, Part I: theory and numerical methods," *Optics Express*, vol. 24, no. 16, pp. 18 353–18 369, 2016.

[29] M. Kamalian, A. Vasylchenkova, D. Shepelsky, J. E. Prilepsky, and S. K. Turitsyn, "Signal modulation and processing in nonlinear fibre channels by employing the Riemann–Hilbert problem," *Journal of Lightwave Technology*, vol. 36, no. 24, pp. 5714–5727, 2018.

[30] B. Deconinck, M. Heil, A. Bobenko, M. Van Hoeij, and M. Schmies, "Computing Riemann theta functions," *Mathematics of Computation*, vol. 73, no. 247, pp. 1417–1442, 2004.

[31] S. Chimmalgi and S. Wahls, "On computing high-dimensional Riemann theta functions," *Communications in Nonlinear Science and Numerical Simulation*, vol. 123, p. 107266, 2023.

[32] M. Kamalian-Kopae, A. Vasylchenkova, D. Shepelsky, J. E. Prilepsky, and S. K. Turitsyn, "Full-spectrum periodic nonlinear Fourier transform optical communication through solving the Riemann-Hilbert problem," *Journal of Lightwave Technology*, vol. 38, no. 14, pp. 3602–3615, 2020.

[33] V. Kotlyarov and D. Shepelsky, "Planar unimodular Baker-Akhiezer function for the nonlinear Schrödinger equation," *Annals of Mathematical Sciences and Applications*, vol. 2, no. 2, pp. 343–384, 2017.

[34] D. Shepelsky, I. Karpenko, S. Bogdanov, and J. E. Prilepsky, "Periodic finite-band solutions to the focusing nonlinear Schrödinger equation by the Fokas method: inverse and direct problems," *Proceedings of the Royal Society A*, vol. 480, no. 2286, p. 20230828, 2024.

[35] F. Musumeci, C. Rottondi, A. Nag, I. Macaluso, D. Zibar, M. Ruffini, and M. Tornatore, "An overview on application of machine learning techniques in optical networks," *IEEE Communications Surveys & Tutorials*, vol. 21, no. 2, pp. 1383–1408, 2018.

[36] P. J. Freire, Y. Osadchuk, B. Spinnler, A. Napoli, W. Schairer, N. Costa, J. E. Prilepsky, and S. K. Turitsyn, "Performance versus complexity study of neural network equalizers in coherent optical systems," *Journal of Lightwave Technology*, vol. 39, no. 19, pp. 6085–6096, 2021.

[37] O. Sidelnikov, A. Redyuk, and S. Sygletos, "Equalization performance and complexity analysis of dynamic deep neural networks in long haul transmission systems," *Optics Express*, vol. 26, no. 25, pp. 32 765–32 776, 2018.

[38] M. Kamalian-Kopae, A. Vasylchenkova, O. Kotlyar, M. Pankratova, J. Prilepsky, and S. Turitsyn, "Artificial neural network-based equaliser in the nonlinear Fourier domain for fibre-optic communication applications," in *2019 Conference on Lasers and Electro-Optics Europe & European Quantum Electronics Conference (CLEO/Europe-EQEC)*. IEEE, 2019, pp. 1–1.

[39] R. T. Jones, S. Gaiarin, M. P. Yankov, and D. Zibar, "Time-domain neural network receiver for nonlinear frequency division multiplexed systems," *IEEE Photonics Technology Letters*, vol. 30, no. 12, pp. 1079–1082, 2018.

[40] W. Q. Zhang, T. H. Chan, and S. A. Vahid, "Serial and parallel convolutional neural network schemes for NFDM signals," *Scientific Reports*, vol. 12, no. 1, p. 7962, 2022.

[41] O. Kotlyar, M. Kamalian-Kopae, J. E. Prilepsky, M. Pankratova, and S. K. Turitsyn, "Machine learning for performance improvement of periodic NFT-based communication system," in *45th European Conference on Optical Communication (ECOC 2019)*. IET, 2019, pp. 1–4.

[42] S. Bogdanov, D. Shepelsky, A. Vasylchenkova, E. Sedov, P. J. Freire, S. K. Turitsyn, and J. E. Prilepsky, "Phase computation for the finite-genus solutions to the focusing nonlinear Schrödinger equation using convolutional neural networks," *Communications in Nonlinear Science and Numerical Simulation*, vol. 125, p. 107311, 2023.

[43] S. Bogdanov, J. E. Prilepsky, D. Shepelsky, M. Kamalian-Kopae, A. Vasylchenkova, E. Sedov, and S. K. Turitsyn, "Fiber-optic communications based on finite-genus solutions to the NLS with a convolutional neural network receiver," in *49th European Conference on Optical Communications (ECOC 2023)*, vol. 2023. IET, 2023, pp. 467–470.

[44] E. V. Sedov, P. J. Freire, V. V. Seredin, V. A. Kolbasin, M. Kamalian-Kopae, I. S. Chekhovskoy, S. K. Turitsyn, and J. E. Prilepsky, "Neural networks for computing and denoising the continuous nonlinear Fourier spectrum in focusing nonlinear Schrödinger equation," *Scientific Reports*, vol. 11, no. 1, p. 22857, 2021.

[45] M. Pelikan, D. E. Goldberg, E. Cantú-Paz *et al.*, "Boa: The Bayesian optimization algorithm," in *Proceedings of the genetic and evolutionary computation conference GECCO-99*, vol. 1. Citeseer, 1999, pp. 525–532.

[46] G. P. Agrawal, *Fiber-optic communication systems*, 4th ed. John Wiley & Sons, 2012, vol. 7.4.1.

[47] E. Agrell and M. Secondini, "Information-theoretic tools for optical communications engineers," in *2018 IEEE Photonics Conference (IPC)*. IEEE, 2018, pp. 1–5.

[48] P. J. Freire, J. E. Prilepsky, Y. Osadchuk, S. K. Turitsyn, and V. Aref, "Deep neural network-aided soft-demapping in coherent optical systems: Regression versus classification," *IEEE Transactions on Communications*, vol. 70, no. 12, pp. 7973–7988, 2022.

[49] Q. Zhang and F. R. Kschischang, "Correlation-aided nonlinear spectrum detection," *Journal of Lightwave Technology*, vol. 39, no. 15, pp. 4923–4931, 2021.